

# Superconducting thick films prepared *via* electrodeposition†

M. S. Martín-González,‡ J. García-Jaca, E. Morán and M. Á. Alario-Franco\*

Depto. Química Inorgánica, Facultad Ciencias Químicas, Universidad Complutense, 28040-Madrid, Spain. E-mail: maaf@eucmax.sim.ucm.es.

Received 28th April 1998, Accepted 8th July 1998

Electrodeposition techniques provide a way of synthesising oxide superconductor thick films in two steps: (a) electrodeposition of the cations and (b) oxidation of the deposit at high temperatures. This method is fast, economic and enjoys the benefits of a well known technology. We have performed the preparation of several copper

ilar papers at [core.ac.uk](http://core.ac.uk)

thermal annealing. Characterisation of the initial deposit and the final superconducting oxide was made by means of infrared spectroscopy, thermal analysis, X-ray diffraction and scanning electron microscopy. The best critical current ( $J_c$ ) values, in  $A\ cm^{-2}$ , for the different phases were:  $YBa_2Cu_3O_{7-\delta}$  (13 000/5 K and 400/77 K),  $Bi_2Sr_2CaCu_2O_{8+\delta}$  (12 000/77 K) and  $Ba_{1-x}K_xBiO_3$  (2 700/5 K).

## Introduction

Electrodeposition has often been used as a promising route to the fabrication of HTSC films since it holds great promise for device development owing to the possibility of film formation on different geometric surfaces and various substrates. Apart from these advantages, this old form of electrochemistry presents other attractive features for the synthesis of superconducting films, such as a low processing time, easy technology transfer to industry and relatively low cost equipment.

Typically, an optimised electrolytic solution containing the suitable ionic species in the appropriate ratio is employed to deposit the cations onto the surface of an electrode. This precursor coating has then to be transformed by an adequate thermal treatment into the desired superconducting phase. Many efforts have of late been made in order to understand and improve the physical and chemical characteristics of the electrodeposition of superconducting materials. These efforts have been focused on making thick films of  $Ba-K-Bi-O$ ,<sup>1</sup>  $Bi-Sr-Ca-Cu-O$ ,<sup>2-7</sup>  $Hg-Ba-Ca-Cu-O$ ,<sup>8</sup>  $Tl-Ba-Ca-Cu-O$ ,<sup>9-16</sup> and  $Y-Ba-Cu-O$ .<sup>17-29</sup> The different variables affecting the electrodeposition process can be classified into four groups: (a) composition of the electrolytic bath, (b) substrate type, (c) the electrodeposition process and (d) thermal treatment.

Different types of solvent have been employed for the preparation of the electrolytic bath including aqueous<sup>17,26</sup> and non-aqueous media, such as dimethylformamide (DMF),<sup>6</sup> isopropanol,<sup>29</sup> dimethyl sulfoxide (DMSO),<sup>1,4,5,8-18</sup> etc. Deposits obtained from non-aqueous baths are more uniform than those from aqueous ones due to the fact that the reduction potential of  $H_2O$  is higher than those of the alkaline-earth metals present in the high- $T_c$  superconductors. Consequently, the formation of a gas at the substrate surface influences the morphology and covering of the deposit. In fact, lower and broader transition temperatures have been observed,<sup>22</sup> when water has been used as solvent. The best results have been obtained for DMSO, because it has a relatively high relative permittivity and is sufficiently resistant to both oxidation and

reduction, so providing a fairly wide working potential range.<sup>30</sup> Besides, the bath composition of metal ions should be adjusted empirically for any given condition by trial and error, because the deposit composition strongly depends on the concentration of the metals present in the bath. An alternative to this general procedure is the use of complexing agents, such as  $CN^-$ ,<sup>23-25</sup> etc.

Two distinct types of electrodeposition process are used: dc electrodeposition<sup>1,4,5,8,24</sup> and pulsed electrodeposition.<sup>9,10,12,13,15,28</sup> The former is the most common, but it has been reported that the latter enhances the electrical, magnetic, mechanical and structural properties of the superconducting film. However, the simultaneous co-electrodeposition of all the cations<sup>4-26,29</sup> and an alternating sequential electrodeposition<sup>2,3,27</sup> can also be used. In the former, the potential is fixed and the cations are deposited all together from the same bath. In the latter, cations are deposited in layers from different baths and a suitable potential can be used to deposit each metal. In this way, good control of the cation ratio in the deposit can be achieved. The influence of the deposition time has also been studied.

Different substrates have been used:  $Ag$ ,<sup>1-4,6,8-13,23-27</sup>  $Au$ ,<sup>14</sup>  $Ni$ ,<sup>18,21</sup>  $Pt$ ,<sup>21</sup>  $Cu$ ,<sup>17,21,22</sup> alloys,<sup>31</sup>  $MgO/Ag$ ,<sup>5,14,15,17,28</sup>  $SrTiO_3/Ag$ ,<sup>15,19</sup>  $ZrO_2/Ag$ ,<sup>14,18</sup> this type of study is very important for the formation of good quality superconducting films because the substrate should not diffuse or chemically react with the deposited film and, even if it diffuses to a small extent, it should not alter the properties of the superconducting state. The influences of the oxidation temperature, heating time and annealing of the thick films have been reported.<sup>2</sup>

Nevertheless, to our knowledge, the available information about the way these film are formed is scarce. This information is crucial for the understanding of the problems observed in the synthesis and, eventually, for their solution. This paper describes the characterisation and superconducting properties of  $Bi_2Sr_2CaCu_2O_{8+\delta}$ ,  $YBa_2Cu_3O_{7-\delta}$ ,  $Ba_{1-x}K_xBiO_3$  thick films prepared *via* an electrodeposition process and thermal treatment. In particular, the composition of the precursor films and their thermal evolution are emphasised.

## Experimental

Films were deposited from a solution of reagent grade metal nitrates in dimethyl sulfoxide (DMSO). The electrodeposition process was carried out in a conventional three-electrode cell.

†Basis of the presentation given at Materials Chemistry Discussion No. 1, 24–26 September 1998, ICMCB, University of Bordeaux, France.

‡Also at Depto. Química Inorgánica y Materiales, Facultad Ciencias Experimentales y Técnicas, Universidad San Pablo-CEU, 28668 Boadilla del Monte, Madrid, Spain.

As a general rule, the reference electrode was Ag/AgCl, the counter electrode was Pt and the working electrode was a silver foil plate ( $0.5 \times 1.0 \text{ cm}^2$ ).  $\text{Al}_2\text{O}_3$  powder was used to clean both sides of the substrate for 1 min each. Then, the films were washed several times using ultrasound within, consecutively, Millipore water and dichloromethane. The co-electrodeposition potential was fixed at  $-3.5 \text{ V}$  vs. Ag/AgCl. The particular synthesis conditions (at room temperature) used for each of the superconducting materials prepared are summarised in Table 1. All the reactants were of a purity grade higher than 99%. Note that owing to the different electrochemical characteristics of the ions, in order to obtain the required film stoichiometry, the composition of the bath has to be optimised; the particular composition determined and the voltage used in each case appear in Table 1. Once the precursor film was deposited, it was oxidised under the conditions also reported in Table 1.

A VersaStat potentiostat/galvanostat Model 253 with a PC computer interface was used for controlling the electrolytic process. A black, amorphous film containing a mixture of phases with the constituent elements of the superconductor is obtained in all cases. The thermal oxidation process was studied by thermogravimetric analysis (TG), using a Perkin Elmer Model 7, and by IR spectroscopy (FTIR), using FTIR Nicolet Magna 550 and Midac Prospect-IR FTIR PRS-INT instruments. The characterisation of the films by X-ray diffraction (XRD) was done using a Siemens D-5000 powder diffractometer. EDS microanalysis and morphological examination were carried out using a JEOL-JSM 6400 scanning electron microscope (SEM).

Superconducting temperatures and the  $M(H)$  loops were recorded using a Quantum Design MPMS XL SQUID magnetometer. The critical current densities in  $\text{A cm}^{-2}$  were obtained, for a slab plane geometry, using the Bean model.<sup>32,33</sup>

## Results and discussion

### Characterisation of the precursor films

The study of the composition of the films at the different preparation stages (electrodeposition, thermal treatment) is a prerequisite for the optimisation of their superconducting properties. According to this idea, the superconducting thick films of  $\text{YBa}_2\text{Cu}_3\text{O}_{7-x}$  (YBC),  $\text{Bi}_2\text{Sr}_2\text{CaCu}_2\text{O}_{8+\delta}$  (BSCC) and  $\text{Ba}_{1-x}\text{K}_x\text{BiO}_3$  (BKB) were analysed by XRD, FTIR and TG.

After the electrodeposition, the precursor films contain different species, as can be deduced from the FTIR data (Fig. 1). Characteristic bands of dimethyl sulfoxide, water and carbonates were observed in the spectra of all precursors (YBC, BSCC and BKB). DMSO and water species are obviously provided by the electrolyte while the carbonate is incorporated from the atmosphere. Water is incorporated into the electrolytic bath by the hydrated salts employed (Table 1) and as an impurity of the DMSO (0.2%) which was used as received. Although the decomposition of water occurs under the working conditions, the characteristic bands of hydroxides

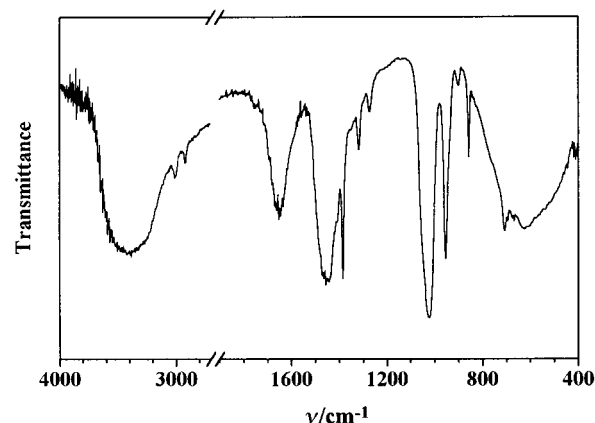


**Fig. 1** FTIR spectra of a representative precursor film. Observed bands:  $3564 \text{ cm}^{-1}$  [ $\nu(\text{H}_2\text{O})$ ],  $3008$  and  $2917 \text{ cm}^{-1}$ , [ $\rho_r(\text{C-H})$ ],  $1651$  [ $\delta(\text{H}_2\text{O})$ ],  $1455$  [ $\nu(\text{CO}_3^{2-})$ ],  $1317 \text{ cm}^{-1}$ , [ $\nu_s(\text{S-CH}_3)$ ],  $1022$  [ $\nu(\text{S=O})$ ] and  $953 \text{ cm}^{-1}$ , [ $\rho_r(\text{CH}_3)$ ].

were not observed. Solvent molecules can be removed from the precursor film by heating at temperatures in the range  $60$ – $110^\circ\text{C}$  for 2–6 h or at room temperature for 72 h. Our results prove that heating the precursors when they are still wet causes the partial decomposition of DMSO, yielding a thin yellow layer of sulfur over the precursor film. In order to minimise the presence of sulfur, evaporation at room temperature was preferred, despite the fact that in this way carbonate formation is enhanced. Under these experimental conditions, carbonates are more reactive than sulfates. For example, on heating YBC films containing carbonates and a small amount of sulfur, barium carbonate is decomposed to yield barium sulfate at  $700^\circ\text{C}$ , which is still present in the final superconducting film as a minor impurity.

From the XRD data (Fig. 2) we can conclude that in the BSCC precursor no phase could be identified while in the data of the BKB film precursors the pattern of metallic bismuth was apparent; on the other hand, in the case of YBC, metallic copper and  $\text{Cu}_2\text{O}$  were found. Note that the metallic phases of copper and bismuth were the only ones identified in the precursor films. These elements are less reactive than the others present in the actual materials and, as a consequence, show a lower tendency to oxidation. Nevertheless, some copper was also detected as copper(I) oxide,  $\text{Cu}_2\text{O}$ , which is indicative of partial oxidation.

Notwithstanding the results of YBC and BKB precursor films, the XRD data of BSCC films did not show the presence of bismuth or copper metallic phases. As was mentioned in the Experimental section, the BSCC precursor films were obtained using pulsed chronoamperometry while YBC and BKB films were prepared by continuous chronoamperometry. Taking into account that the TG curves (*vide infra*) of BSCC films were clearly indicative of the presence of metallic bismuth and very similar to those of YBC and BKB films, it could be

**Table 1** Synthesis conditions for the  $\text{Bi}_2\text{Sr}_2\text{CaCu}_2\text{O}_{8+\delta}$ ,  $\text{YBa}_2\text{Cu}_3\text{O}_{7-\delta}$  and  $\text{Ba}_{1-x}\text{K}_x\text{BiO}_3$  phases

Superconducting phase	Bath composition	Deposition conditions (vs. Ag/AgCl)	Thermal treatment
$\text{Bi}_2\text{Sr}_2\text{CaCu}_2\text{O}_{8+\delta}$	20 mM $\text{Bi}(\text{NO}_3)_3 \cdot 5\text{H}_2\text{O}$ 20 mM $\text{Sr}(\text{NO}_3)_2$ 13 mM $\text{Ca}(\text{NO}_3)_2 \cdot 4\text{H}_2\text{O}$ 15 mM $\text{Cu}(\text{NO}_3)_2 \cdot 3\text{H}_2\text{O}$	Pulsed electrodeposition $-3.5 \text{ V}/30 \text{ s} + 0 \text{ V}/30 \text{ s}$	$800^\circ\text{C}$ , 24 h, air
$\text{YBa}_2\text{Cu}_3\text{O}_{7-\delta}$	20 mM $\text{Y}(\text{NO}_3)_3$ 36 mM $\text{Ba}(\text{NO}_3)_2$ 44 mM $\text{Cu}(\text{NO}_3)_2 \cdot 3\text{H}_2\text{O}$	dc electrodeposition $E = -3.5 \text{ V}/30 \text{ min}$	$900^\circ\text{C}$ , 24 h, air $+450^\circ\text{C}$ , 24 h, $\text{O}_2$ Slow cooling
$\text{Ba}_{1-x}\text{K}_x\text{BiO}_3$	9.5 mM $\text{Ba}(\text{NO}_3)_2$ 20 mM $\text{Bi}(\text{NO}_3)_3 \cdot 5\text{H}_2\text{O}$ 3 mM $\text{KNO}_3$	dc electrodeposition $E = -3.5 \text{ V}/30 \text{ min}$	$700^\circ\text{C}$ , 72 h, air Slow cooling

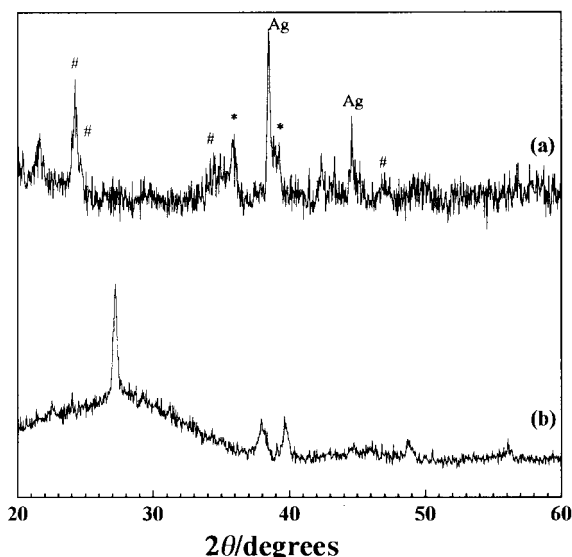


Fig. 2 XRD diffractograms of (a) YBC and (b) BKB precursor films. (#)=BaCO<sub>3</sub>, (\*)=CuO.

concluded that the employed electrodeposition method is more related to the crystallinity of the precursor films than to its composition. Pulsed electrodeposition requires an alternating change from  $-3.5$  V (reducing potential) to  $0$  V vs. Ag/AgCl (slightly oxidising potential under our experimental conditions) in a square-type wave that is cycled about 120 times in the preparation of the film. Under these synthesis conditions, the highly crystalline phases are not favoured.

In none of the precursor films was the presence of phases containing alkaline-earth elements detected. These elements are very reactive in their metallic form and, consequently, particularly unstable in air. Owing to the presence of water in the electrolyte, it is suggested that the alkaline-earth metals react with water during the electrodeposition process to give oxidised phases. During the evaporation process, these oxides can react with atmospheric CO<sub>2</sub> to yield carbonates, which were detected during the thermal treatment of the films.

In spite of the complicated composition of the precursor films the operation under ambient conditions reduces notably the cost of the large-scale manufacture of these thick films and makes electrodeposition a useful technique. Some authors have used anhydrous conditions to electrodeposit films under inert conditions<sup>4</sup> or for the preparation of metallic alloys by different metal forming processes<sup>34</sup> in order to improve the quality of the film. We have proved that this can be also achieved *via* substrate cleaning or *via* a pressure treatment of the precursor films.<sup>25,35</sup>

The evolution of the precursors during the thermal treatment was followed by means of TG and, in order to elucidate the thermogravimetric processes, TG was also performed on different mixtures of two of the corresponding metals (Cu:Ba, Cu:Sr, Bi:Ca, Bi:Sr, Bi:Cu) prepared by electrodeposition. The initial weight losses detected in the thermograms can be attributed to the adsorbed gases that evolve at low temperatures and their magnitude depends on the evaporation process employed (*vide supra*). Interestingly, all the precursors that contain bismuth showed a characteristic weight gain in the range  $257$ – $322$  °C. This process is due to the oxidation of bismuth and its reaction temperature seems to be influenced by the other elements present in the precursor film.

The thermogravimetric processes observed in the range  $405$ – $503$  °C are assigned to the decarbonation of the alkaline-earth phases. However, the thermogravimetric behaviour of each particular phase could not be unambiguously inferred from the available data. The mass evolved is rather more

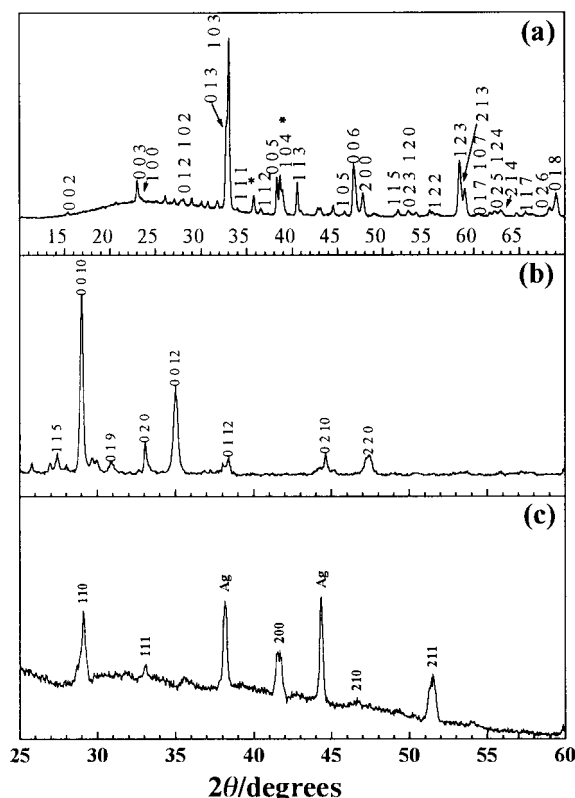


Fig. 3 XRD patterns of the deposits of (a) YBC, (b) BSCC and (c) BKB materials.

dependent on the exposure time of the precursor film during the evaporation of the solvent than on its initial composition.

The characterisation of the final material was performed by XRD (Fig. 3). The corresponding diffractograms confirm the presence of the respective superconducting materials, and some minor impurities in the cases of YBC and BSCC.

### Morphology of the films

The morphology of the deposits is important in the understanding of the magnitude of superconducting properties such as the critical current density,  $J_c$ . For that reason, representative films of different superconductors were observed by SEM. The results showed that the morphology depends on both the composition and the history of the films.

The morphology of the films before the oxidative heating consists of a mixture of particles with a variety of sizes, shapes and contrast types [Fig. 4(a)]. The film surface is covered with clusters of rounded particles, with clear contrast in the micrograph, which were only observed at the surface. These particles are those most exposed to air and, consequently, are likely to contain an important amount of carbonates and adsorbed gases such as H<sub>2</sub>O and CO<sub>2</sub>. Underneath these clusters, a rough layer of grains is observed. This roughness is caused by the dendritic growth of the films and the loss of the solvent mixture (mainly DMSO) during the evaporation process. As can be seen, the overall morphology of the thick precursor films obtained is spongy, but can be partially optimised by pressing the precursors before the thermal treatment.<sup>25,35</sup>

During the oxidative heating the morphology of the films undergoes a crucial change that depends on the prepared superconductor.

(1) In the case of BKB, the deposits mimic the shape of the silver substrate<sup>1</sup> and are formed by a mosaic of compact blocks that are closely packed [Fig. 4(b)]. In spite of this good local covering, the overall cover was relatively poor with an average film thickness of  $5$  μm. The deposit was concentrated

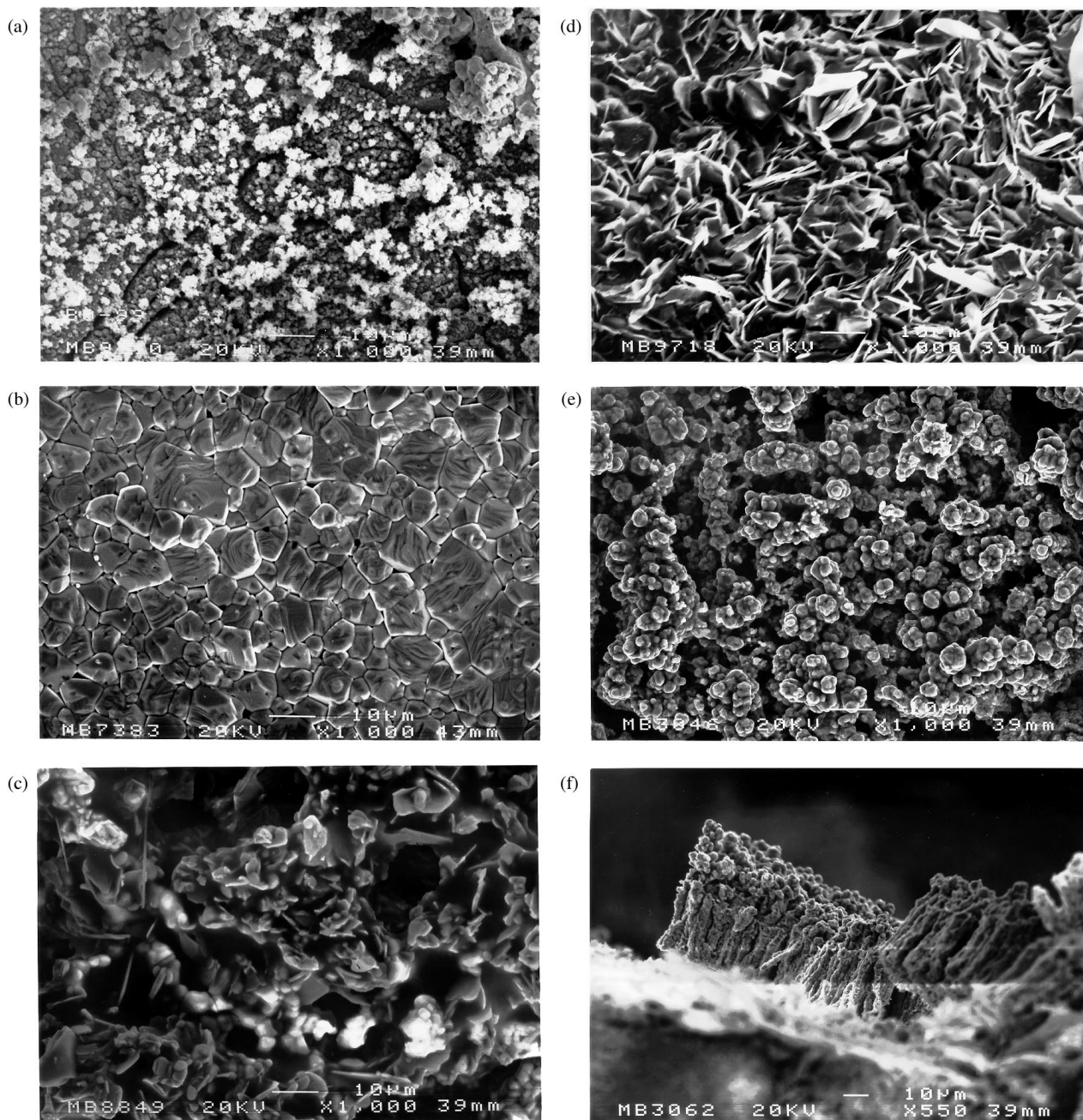


**Fig. 4** Micrographs of (a) precursor film and superconducting thick films of (b) BKB, (c) BSCC, (d) BSCC (with pressure treatment) and YBC (e) top view and (f) side view.

in small areas over the substrate with the shape shown in Fig. 4(b) which is similar to those reported for BKB thin films prepared by the more elaborate molecular beam epitaxy technique.<sup>36</sup>

(2) The BSCC deposits exhibit the characteristic plate-like particles of  $\text{Bi}_2\text{Sr}_2\text{CaCu}_2\text{O}_{8+\delta}$  samples with a size of about 5  $\mu\text{m}$ . A general tendency of these particles to sit perpendicular to the  $c$ -axis was noticed in the observed films [Fig. 4(c)]. The films are not continuous, but the connectivity between grains could be markedly improved by the application of pressure to the precursor films: in fact, when the precursor films, after evaporation in air, were pressed at 14 kbar for 5 min, the subsequent oxidative thermal heating yielded a deposit with bigger particles (about 10–20  $\mu\text{m}$ ) and a more uniform morphology [Fig. 4(d)].

(3) Fig. 4(e) shows a representative micrograph of the YBC thick films obtained in this study. In contrast to the precursor, the particles have a unique shape and are grouped in columns which are not connected at the top. A side view of the film

[Fig. 4(f)], displays the arrangement of those 'columns' in the film. The material which was deposited at the end of the process (top of the columns) does not show continuity and will necessarily give poor transport properties. However, in the middle and lower parts, the connectivity and, consequently, the transport is enhanced. Of the three types of superconducting thick films prepared, the YBC material gave the best covering and the thickest layer (40  $\mu\text{m}$ ).

### Superconducting properties

The critical temperatures characteristic of the different films are collected in Table 2. It can be seen that these values are comparable to those observed in the literature and indicate that all the films are superconducting. Obviously, the critical current density is also important in many of the eventual applications of the superconducting films.

For the results obtained for the BKB films produced by electrodeposition, there do not seem to be equivalent data in

**Table 2** Summary of the superconducting properties of electrodeposited films of Ba–K–Bi–O, Bi–Sr–Ca–Cu–O, Hg–Ba–Ca–Cu–O (1223), Tl–Ba–Ca–Cu–O, Y–Ba–Cu–O phases

HTSC film	$T_c$ /K	$J_c/A\text{ cm}^{-2}$	Ref.
Ba–K–Bi–O	35	—	1
	35	2 700/5 K	This work
Bi–Sr–Ca–Cu–O	52–79	400/60 K	7
	82	15 000/77 K	2
	84	33 000	3
	85	300–400	5
	95	4 300/77 K	This work <sup>a</sup>
	95	12 000/77 K	This work <sup>b</sup>
Hg–Ba–Ca–Cu–O	114	—	8
Tl–Ba–Ca–Cu–O	—	44 200/77 K	9
	106	14 630	10
	110	19 600	13
	102	10 <sup>5</sup> /77 K	11
Y–Ba–Cu–O	78	5 160	28
	82	6 600	27
	91	4 000	18
	91	5 160	19
	92	3 000/77 K	23
	92	2 908/4.2 K	25
	92	51/77 K	26
	92	400/77 K	This work
	92	13 000/5 K	This work

<sup>a</sup>Without pressuring the precursor film. <sup>b</sup>Applying a pressure of 14 kbar for 5 min.

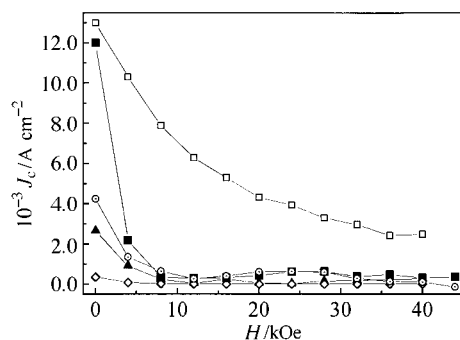


**Fig. 5**  $J_c$  values of the different films: (□) YBC at 5 K, (■) BSCC with pressure at 77 K, (○) BSCC without pressure at 77 K, (▲) BKB at 5 K and (◇) YBC at 77 K.

the literature. The  $J_c$  values obtained at 5 K and in zero applied field (ZF), 3000 A cm<sup>-2</sup>, are markedly reduced by the application of a magnetic field: 700 A cm<sup>-2</sup> at 500 Oe and 150 A cm<sup>-2</sup> at 1000 Oe. Nevertheless, films obtained by much more expensive techniques like molecular beam epitaxy display  $J_c$  values up to 10<sup>5</sup> A cm<sup>-2</sup>. There is certainly much room for improvement in here.

When pressure is applied to the BSCC precursor film an improvement is observed in the  $J_c$  value. In this way, the critical density current is four times higher than the one obtained without pressure. These results are comparable to those reported in the literature obtained by other techniques.<sup>37</sup> However, the  $J_c$  data at ZF drop to 27% without applied pressure and to 14% with pressure (Fig. 5) in accordance with the literature.<sup>37</sup> Yet, in both cases,  $T_c$  is rather high, ca. 95 K.

The YBC films can be considered satisfactory, taking into account the wide range of  $J_c$  results that have been reported in the literature as far as electrodeposition is concerned. At 5 K and ZF the  $J_c$  values obtained are 40 times higher than those obtained at 77 K ZF and, with an applied field of 500 Oe, they are about 100 times higher. Comparing the results obtained at the same temperature, note that the  $J_c$  values at ZF (5 K) are reduced to 75% when a magnetic field of 500 Oe is applied (Fig. 5). However, better results have been obtained by other methods owing to an improvement in texture.<sup>37</sup>

## References

- M. S. Martín-González, J. García-Jaca, E. Morán and M. Á. Alario-Franco, *Physica C*, 1998, **297**, 185.
- Ph. Gendre, L. Schmirgeld-Mignot, P. Régnier, S. Sénoussi, K. Frikach and A. Marquet, *Physica C*, 1994, **235–240**, 953.
- F. Legendre, L. Schmirgeld-Mignot, P. Régnier, Ph. Gendre and S. Sénoussi, *Appl. Supercond.*, 1995, **148**, 339.
- K. A. Richardson, D. M. W. Arrigan, P. A. J. de Groot, P. C. Lanchester and P. N. Bartlett, *Electrochim. Acta*, 1996, **41**, 1629.
- M. Maxfield, H. Eckhardt, Z. Iqbal, F. Reidinger and R. H. Baughman, *Appl. Phys. Lett.*, 1989, **54**, 1932.
- V. N. Shinde and S. H. Pawar, *Indian J. Phys. A*, 1994, **68**, 423.
- Y. C. Kim, H. N. You, S. K. Han, M. S. Jang and P. H. Hur, *Physica C*, 1991, **185–189**, 2303.
- S. H. Pawar, M. J. Ubale and S. B. Kulkarni, *Mater. Lett.*, 1994, **20**, 279.
- R. N. Bhattacharya, A. Duda, D. S. Ginley, J. A. DeLuca, Z. F. Ren, C. A. Wang and J. H. Wang, *Physica C*, 1994, **229**, 145.
- R. N. Bhattacharya and R. D. Blaugher, *Physica C*, 1994, **225**, 269.
- R. N. Bhattacharya and R. D. Blaugher, *Physica C*, 1994, **229**, 244.
- R. N. Bhattacharya, A. Duda, D. S. Ginley, J. A. DeLuca, Z. F. Ren, C. A. Wang and J. H. Wang, *Physica C*, 1994, **229**, 145.
- R. N. Bhattacharya and M. Paranthaman, *Physica C*, 1995, **251**, 105.
- L. Y. Su, C. R. M. Grovenor and M. J. Goringe, *Supercond. Sci. Technol.*, 1994, **7**, 133.
- R. N. Bhattacharya, P. A. Parilla and R. D. Blaugher, *Physica C*, 1993, **211**, 475.
- K. A. Richardson, P. A. J. de Groot, P. C. Lanchester, P. R. Birkin and P. N. Bartlett, *J. Electroanal. Chem.*, 1997, **420**, 21.
- D. J. Zurawski, P. J. Kulesza and A. Wieckowski, *J. Electrochem. Soc.*, 1988, **136**, 1607.
- R. N. Bhattacharya, R. Noufi, L. L. Roybal and R. K. Ahrenkiel, *J. Electrochem. Soc.*, 1991, **138**, 1643.
- R. N. Bhattacharya, P. A. Parilla, R. Noufi, P. Arendt and N. Elliott, *J. Electrochem. Soc.*, 1992, **139**, 67.
- H. Minoura, K. Naruto, H. Takano, E. Haseo, T. Sugiura, Y. Ueno and T. Endo, *Chem. Lett.*, 1991, **3**, 379.
- N. Casañ-Pastor, P. Gómez-Romero, A. Fuentes, M. R. Palacín, J. M. Navarro and M. Brossa, in *Superconductivity in Spain* (MIDAS Program, ed. F. Yndurain, MIDAS Program Manager, Madrid), 1993, p. 87.
- P. Slezak and A. Wieckowski, *J. Electrochem. Soc.*, 1991, **138**, 1038.
- S. Ondoño-Castillo, V. Gomis and N. Casañ-Pastor, *Proceedings of the V Reunión Nacional de Materiales*, ed. M. Domínguez, Unidad Especializada de Ciencias y Tecnología de Materiales y Departamento de Física de la Materia Condensada, Universidad de Cádiz, Cádiz, 1996, p. 105.
- S. Ondoño-Castillo, F. Pérez, A. Fuentes, P. Gómez-Romero and N. Casañ-Pastor, *Physica C*, 1994, **341**, 235 (Proceedings of the M2S-HTSC IV, Grenoble, 1994).
- S. Ondoño-Castillo and N. Casañ-Pastor, *Physica C*, 1997, **276**, 251.
- S. Ondoño-Castillo, A. Fuentes, F. Pérez, P. Gómez-Romero and N. Casañ-Pastor, *Chem. Mater.*, 1995, **7**, 771.
- P. Régnier, S. Poissonnet, G. Villars and C. Louchet, *Physica C*, 1997, **282–287**, 2575.
- R. N. Bhattacharya, P. A. Parilla, A. Mason, L. L. Roybal, R. K. Ahrenkiel, R. Noufi, R. P. Hellmer, J. F. Kwak and D. S. Ginley, *J. Mater. Res.*, 1991, **6**, 1389.
- S. B. Abolmaali and J. B. Talbol, *J. Electrochem. Soc.*, 1993, **140**, 443.
- J. N. Butler, *J. Electroanal. Chem.*, 1967, **14**, 89.
- M. S. Martín-González, J. García-Jaca, E. Morán and M. Á. Alario-Franco, *Bol. Soc. Esp. Ceram. Vidrio*, 1998, **37**, 200.
- C. P. Bean, *Phys. Rev. Lett.*, 1964, **8**, 250.
- A. P. Malozemoff, in *Physical Properties of High Temperature Superconductors I*, ed. D. M. Ginsberg, World Scientific, Singapore, 1989, p. 73.
- W. Gao and J. B. Vander Sande, *J. Phys. IV*, 1993, **3**, 187.
- M. S. Martín-González, J. García-Jaca, E. Morán and M. A. Alario-Franco, *J. Mater. Res.*, submitted.
- E. S. Hellman, E. H. Hartford and E. M. Gyorgy, *Appl. Phys. Lett.*, 1991, **58**, 1335.
- N. M. C. Alford, S. J. Penn and T. W. Button, *Supercond. Sci. Technol.*, 1997, **10**, 169.